Applied Mathematical Modelling 36 (2012) 1995–2002

Contents lists available at SciVerse ScienceDirect

Applied Mathematical Modelling

journal homepage: www.elsevier.com/locate/apm

Effects of defects on the effective thermal conductivity of thermal barrier coatings

Shen Wei [a,b], Wang Fu-chi [a], Fan Qun-Bo [a,*], Ma Zhuang [a]

[a] School of Materials Science and Engineering, Beijing Institute of Technology, Beijing 100081, PR China
[b] Central Iron and Steel Research Institute, No. 76 Xueyuan Nanlu, Haidian, Beijing 100081, PR China

ARTICLE INFO

Article history:
Received 27 September 2009
Received in revised form 22 July 2011
Accepted 9 August 2011
Available online 3 September 2011

Keywords:
Defects
TBCs
Effective thermal conductivity
Microstructure

ABSTRACT

It is difficult to establish structure-property relationships in thermal barrier coatings (TBCs) because of their inhomogeneous-geometry microstructures caused by defects. In the current research, the effects of pores and cracks on the effective thermal conductivity of TBCs are studied. Based on the law of the conservation of energy, mathematical formulations are proposed to indicate the relationship between defects and the effective thermal conductivity. In this approach, detailed equations are illustrated to represent the shape and size of defects on the effective thermal conductivity of TBCs. Different from traditional empirical analyses, mixture law or statistical method, for the first time, our results with the aid of finite element method (FEM) and strict analytical calculation show the influence of pore radius and crack length on effective thermal conductivity can be quantified. As an example to a typical microstructure of plasma sprayed TBCs, the effects of defects on the effective thermal conductivity of TBCs are expressed by the influence parameter, which indicating that the longest transverse crack dominates the contribution of the effective thermal conductivity along the spray direction compared with any individual defect.

1. Introduction

It has been shown both experimentally and theoretically that thermal properties are strongly dependent on all kinds of defects in materials [1,2]. The defective microstructures of TBCs greatly influence the effective thermal conductivity and thus influence thermal resistance behaviors. Usually, microscopically defective materials can be equivalently replaced by a macroscopically homogeneous continuum medium with properly defined effective properties [3]. However, effective properties are related to detailed microstructure of inhomogeneities. Depending on the shape and the distribution of the defects, the overall properties of TBCs will possess different degree of anisotropy.

For optimal design, establishing microstructure-property correlations is necessary. There has been extensive analytical and numerical work in establishing relations between thermal conductivity and microstructures for porous media. Hasselman and Singh [4,5] presented expressions for the effect of penny-shaped cracks and micro-cracking on the thermal conductivity of solid materials. In [6], a model without considering reactions between defects provides very good agreement in the thermal conductivity of TBCs between the estimated and experimental values, which indicates the reactions between defects is sufficiently small that can be ignored. Markov and Preziosi [7] reviewed some rigorous method to relate effective properties including thermal conductivity of random porous media through microstructure characterization via statistical correlation function. Nicholls and co-workers [8] reviewed methods capable of lowering the thermal conductivity of

* Corresponding author. Tel.: +86 10 68911144.
E-mail address: fanqunbo@bit.edu.cn (F. Qun-Bo).

0307-904X/$ - see front matter
doi:10.1016/j.apm.2011.08.018

Nomenclature

K	thermal conductivity
K_0	thermal conductivity of the non-defective bulk material
K_{eff}	effective thermal conductivity
∇T	temperature gradient
ΔT	temperature difference
l	width of plate
h	height of plate
q_Γ	total steady-state heat flux per unit thickness
Q_{sum}	total heat power through the plate
ρ	porosity
A	area of nonlinear thermal gradient region around the defect
a	pore radius
b	half of crack length
C_K	an independent variable of nonlinear area around the defect
D	the influence parameter of defects on the effective thermal conductivity

EB-PVD TBCs and identified four significant factors that may lower the coating thermal conductivity by modifying either phonon and/ or photon transport. Lu and Song [9] proposed an expression for the reduced effective thermal conductivity of composites containing randomly distributed spherical inclusions. Sevostianov and Kachanov [10] calculated effective anisotropic thermal conductivities of the plasma sprayed ceramic coating in terms of the relevant microstructural parameters. Considering the reduction in the intrinsic thermal conductivity due to scattering of phonons, the Maxwell theory was used to analyze the thermal conductivity of porous yttria-stabilized zirconia [11]. Clarke [12] estimated the minimum thermal conductivity of insulating materials in the absence of rigorous theories for high-temperature thermal conductivity of TBCs. Nakamura and co-workers [13] have investigated effects of pores and interfaces on effective thermal conductivity of plasma sprayed zirconia coatings, and they found the splat interfaces were as equally important as the porosity in defining the properties of plasma sprayed coatings. Cernuschi and co-workers [14] have studied the effect of porosity on the thermal diffusivity on artificially aged, free-standing thermal TBCs produced by air plasma spray. Also, numerous traditional empirical formulas were applied to calculate to the effective thermal conductivity of coatings [15–17]. Additionally, in [18] and [19], the authors took use of the object-oriented finite element (OOF) method [20] to study the effective thermal conductivity of coatings with actual microstructures, and most of their works only referred to the relationship between porosity and the effective thermal conductivity. All these previous studies provide useful information about fundamental characteristics and methodologies in thermal conductivity analysis of porous materials. However, no detailed mathematical formulation is developed to explain how the shape, size and distribution of defects affect the effective thermal conductivity.

In our previous research [21], new expressions have been proposed to study effects of splat interfaces and defects on effective properties of thermal barrier coatings, and a comparison between effect coefficients of splat interfaces and defects shows that splat interfaces account for about 55–70% of the total reduction in the effective thermal conductivity, which indicates that the splat interfaces have greater influences on the thermal conductivity than defects, quite different from any traditional opinion. In this context, novel mathematical formulas are proposed to indicate the relationship between defects and the effective thermal conductivity of TBCs by the law of the conservation of energy. In the mathematical expression, the effect of nonlinear area around the defect on the effective thermal conductivity is an independent variable determined by the defect itself. For the first time, the effective thermal conductivity affected by the radius of pore and the length of crack is expressed mathematically in detail. Additionally, using the newly developed mathematical expression, we further analyze the contribution of defects to the effective thermal conductivity of a typical TBC microstructure along the spray direction.

2. Mathematical formulation of the effective thermal conductivity affected by defects

2.1. Prediction of the effective thermal conductivity

Thermal conductivity K is the property of a material that indicates its ability to conduct heat. It appears primarily in Fourier's law for heat conduction.

$$q = -K\nabla T, \tag{1}$$

$$\nabla T = n_0 \frac{\Delta T}{dh}, \tag{2}$$

here, ∇T is the temperature gradient, ΔT is the temperature difference and dh is the thickness of conducting surface separating the two temperatures.

The effective thermal conductivity is determined by the steady-state heat transfer analysis. To obtain the effective thermal conductivity along the heat flow direction, a fixed temperature difference is set between the top and the bottom boundaries, and the other two boundaries are kept insulated. Thus, the effective in-plane thermal conductivity, K_{eff}, in the heat flow direction can be computed with Fourier's equation:

$$K_{eff} = \frac{q_\Gamma \cdot h}{\Delta T \cdot l}. \tag{3}$$

Here, q_Γ is the total steady-state heat flux per unit thickness through any transverse cross-section of the model. h and l are the height and width of the model, respectively. It should be emphasized that K_{eff} in this context is determined by defects without considering the influence of splat interfaces. With this assumption, effects of the shape, size and distribution of defects on the thermal conductivity can be clarified more clearly.

2.2. Effects of defects on the effective thermal conductivity

The top and the bottom of a rectangular plate of TBCs with unit thickness are assigned constant temperature of $T + \Delta T$ and T, such that a temperature difference of ΔT is set up across the plate. The other two sides are kept adiabatic. Under steady-state conditions, the total heat power Q_{sum} through TBCs can be computed from Eq. (3):

$$Q_{sum} = K_{eff} \cdot \Delta T \cdot l. \tag{4}$$

If the material of TBCs is isotropic, for plate without defects inside, the heat power is given by Fourier's law as follows

$$Q_{sum} = \int_S K_0 \cdot (\delta \nabla T)^T \nabla T dS = \int_S K_0 \cdot \frac{\Delta T}{dh} dS = K_0 \cdot \frac{\Delta T}{h} \cdot hl = K_0 \cdot \Delta T \cdot l, \tag{5}$$

where K_0 is intrinsic thermal conductivity of the non-defective bulk material. The temperature gradient is equal to $\frac{\Delta T}{dh}$ because of the non-defective plate. Further, Q_{sum} can be rewritten as $K_0 \cdot \Delta T \cdot l$, due to $dS = dh \cdot dl$.

Thus,

$$K_{eff} = K_0. \tag{6}$$

With defects inside of the TBCs plate shown in Fig. 1, the localized effects caused by any internal defect acting on the body will dissipate or smooth out within region A. Furthermore, the resulting thermal gradient distribution at region B far away from the defect will be the same as that caused by any other statically equivalent thermal load applied to the body without

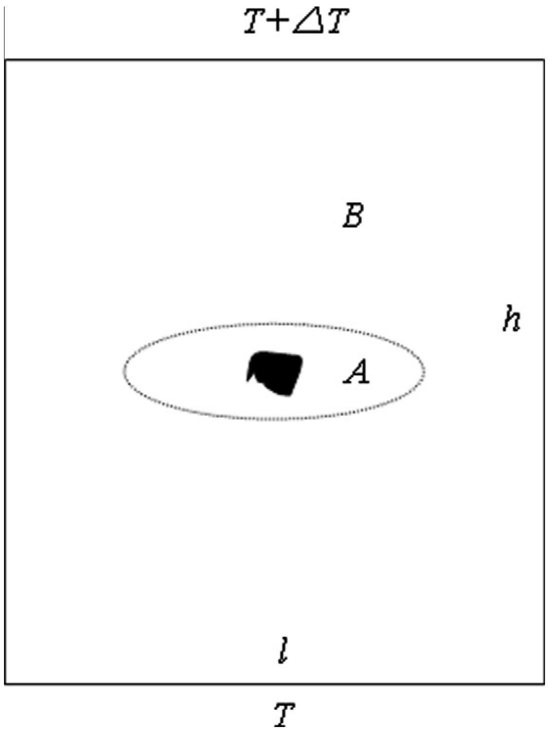

Fig. 1. TBCs plate with defect inside subject to a temperature difference load. The dark color represents defect.

defects inside. Because of the localized effects caused by defect, a nonlinear thermal gradient area (region A) will occur around the defect. Since the thermal conductivity of air is very small as compared to that of the bulk material [13], zero conductivity is assumed within defect areas in our models. The total heat power is rewritten as

$$Q_{sum} = \int_S K_0 \cdot (\delta \nabla T)^T \nabla T dS = \int_B K_0 \cdot \frac{\Delta T}{h} dB + \int_A K_0 \cdot (\delta \nabla T)^T \nabla T dA = K_0 \left\{ \frac{\Delta T}{h} [(1-\rho) \cdot hl - A] + \int_A (\delta \nabla T)^T \nabla T dA \right\}, \tag{7}$$

here, A is a function related to the shape and size of defect, and $\int_A (\delta \nabla T)^T \nabla T dA$ is function related to A and $\frac{\Delta T}{h}$.

According to Eqs. (4) and (7), K_{eff} can be expressed as

$$K_{eff} = K_0 \cdot \left[1 - \rho - \frac{A}{hl} + \frac{\int_A (\delta \nabla T)^T \nabla T dA}{\Delta T \cdot l} \right]. \tag{8}$$

Considered

$$f\left(A, \frac{\Delta T}{h}\right) = \frac{\int_A (\delta \nabla T)^T \nabla T dA}{\frac{\Delta T}{h}}, \tag{9a}$$

$$C_K = f\left(A, \frac{\Delta T}{h}\right) - A. \tag{9b}$$

Thus, the effective in-plane thermal conductivity of TBCs can be simplified as

$$K_{eff} = K_0 \left(1 - \rho - \frac{C_K}{hl} \right), \tag{10}$$

here, C_K is an independent variable only affected by thermal nonlinear area around the defect. Certainly, C_K should be proved to have no relationship with thermal gradient and plate size. To this end, a finite element model of plate with an irregular defect inside is shown in Fig. 2, where the area of the defect with determined shape and size is 0.06564 μm^2, while the size of plate model is changing. The calculated C_K values with different ΔT, l, h are tabulated in Table 1. As seen in Table 1, though ΔT

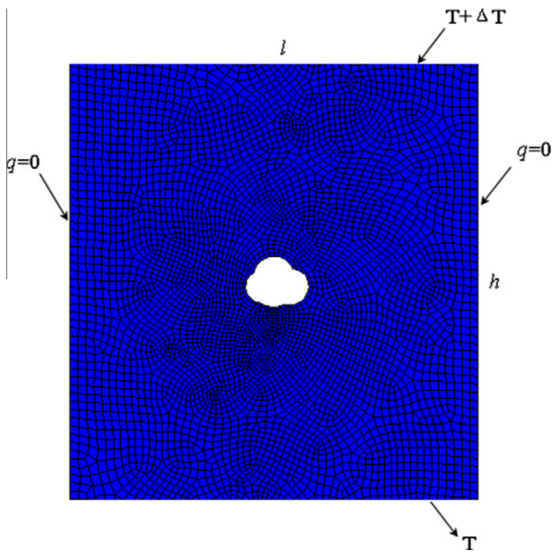

Fig. 2. A finite element model of plate with an irregular defect inside.

Table 1
C_K values with different ΔT, l, h

ΔT (°C)	l (μm)	h (μm)	K_{eff}/K_0	C_K (μm^2)
1	2	2	0.9678	0.06316
10	4	2	0.984	0.06236
100	4	4	0.9919	0.06326
1000	8	8	0.998	0.06236

changes from 1 °C to 1000 °C within different size geometry models, there is no significant change in C_K, and the slight variation of C_K is simply due to the number of mesh elements which might cause somewhat calculation errors. Obviously, the results from FEM analysis show that the ΔT, l, h have no effect on C_K, which is only determined by the defect itself.

If there are n defects and defects are not affected by each other, the effective thermal conductivity of TBCs can be further expressed as follows

$$K_{eff} = K_0\left(1 - \rho - \frac{\sum_{i=1}^{n} C_K(i)}{hl}\right). \tag{11}$$

It is found that if the defects are remote from the boundaries of TBCs and not affected by each other, there is no relationship between the defects location in the TBCs and the effective thermal conductivity.

To better describe the effects of multiple effects on the effective thermal conductivity, the effects of defects on effective thermal conductivity can be described as follows

$$K_{eff} = K_0\left(1 - \frac{D}{hl}\right), \tag{12a}$$

$$D = \rho \cdot hl + \sum_{i=1}^{n} C_K(i). \tag{12b}$$

D is the influence parameter of defects on the effective thermal conductivity, which is between 0 and $h \cdot l$.When there is no defect inside of TBCs, D is 0.

2.3. Effects of defects on the effective thermal conductivity

2.3.1. Effects of pores on the effective thermal conductivity

From Eq. 10, it is found that CK is an independent variable only affected by thermal nonlinear area around the defect. Thus, CK can be further expressed as

$$C_K = \lambda \cdot f(shape) \cdot S(defects), \tag{13}$$

where, λ is the influence factor; $f(shape)$ is a function of the shape of defects; and $S(defects)$ is the area of defects. With different pores radius a, $S(defects) = \pi \cdot a^2$,and $f(shape)$ is a invariable parameter. Based on the above analysis, C_K results with different pore radius a can be written as:

$$C_K = \alpha \cdot a^2. \tag{14}$$

C_K results with v.s. pore radius a from FEM analyses are plotted in Fig. 3a, which indicates that $\alpha \approx 3.06$.

Combining Eq (10) and Eq (14)

$$K_{eff} = K_0\left(1 - \rho - \frac{\alpha \cdot a^2}{hl}\right). \tag{15}$$

If defects are composed of n pores and pores are not affected by each other. The effective thermal conductivity can be expressed as follows

$$K_{eff} = K_0\left(1 - \rho - \frac{\alpha \sum_{i=1}^{n} a_i^2}{hl}\right). \tag{16}$$

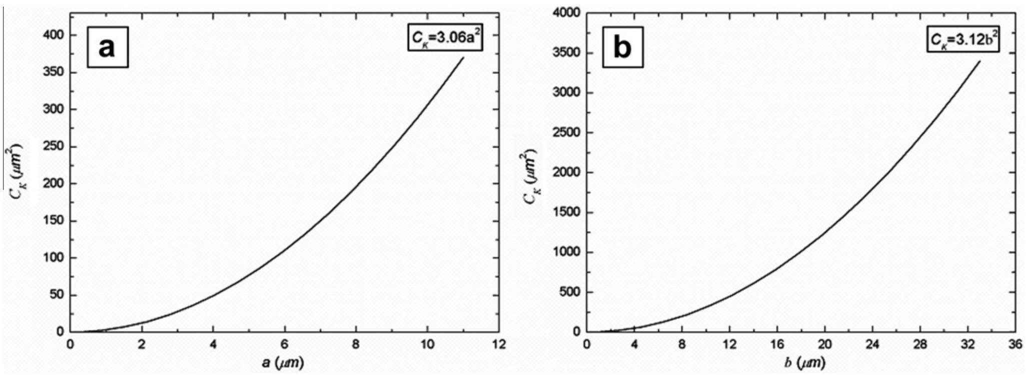

Fig. 3. C_K results from FEM analyses with (a) different pore radiuses. (b) different half of crack lengths. Finite element models of plate with different defects inside are built to obtain C_K values. Some slight varieties of C_K expressions may occur due to the number of mesh elements is somewhat varying with different size of defects and plates.

Hence, the effects of pores on the effective thermal conductivity can be described as

$$D_p = \rho \cdot hl + \alpha \sum_{i=1}^{n} a_i^2. \tag{17}$$

2.3.2. Effects of cracks on the effective thermal conductivity

Consider a transverse crack in an infinite TBCs plate where the crack is parallel with the top of plate. Since the porosity induced by a crack is so small that the porosity ρ can be assumed to be zero, the effective thermal conductivity along the spray direction can be described as

$$K_{eff} = K_0\left(1 - \frac{C_K}{hl}\right). \tag{18}$$

Suppose the shape of different transverse cracks can be simplified as oval with identical curvature. C_K results with different transverse crack length $2b$ can be expressed as:

$$C_K = \beta \cdot b^2 \tag{19}$$

C_K results with different transverse crack length $2b$ from FEM analyses are plotted in Fig. 3b, which shows that $\beta \approx 3.12$.

Combining Eq. (18) and Eq. (19)

$$K_{eff} = K_0\left(1 - \frac{\beta_c \cdot b^2}{hl}\right). \tag{20}$$

Thus, the influence parameter of a transverse crack on the effective thermal conductivity can be described as

$$D_c = \beta \cdot b^2. \tag{21}$$

If defects are composed of n transverse cracks, cracks are not affected by each other. Since the porosity induced by n transverse cracks can not be ignored, the effects of these cracks on the effective thermal conductivity along the spray direction can be expressed as follows

$$K_{eff} = K_0\left(1 - \rho - \frac{\beta_c \sum_{i=1}^{n} b_i^2}{hl}\right). \tag{22}$$

Hence, the influence parameter of n transverse cracks on the effective thermal conductivity can be given by

$$D_C = \rho \cdot hl + \beta \sum_{i=1}^{n} b_i^2. \tag{23}$$

2.3.3. Effects of pores and cracks on the effective thermal conductivity

Suppose the TBCs microstructure is composed of m pores and n transverse cracks, and these defects are not affected by each other. In such case, the effective thermal conductivity along the spray direction can be given by

$$K_{eff} = K_0\left(1 - \rho - \frac{\beta_p \sum_{i=1}^{m} a_i^2 + \beta_c \sum_{j=1}^{n} b_j^2}{hl}\right). \tag{24}$$

Hence, the influence parameter of defects on the effective thermal conductivity can be described as

$$D = \rho \cdot hl + \alpha \sum_{i=1}^{m} a_i^2 + \beta \sum_{j=1}^{n} b_j^2 \tag{25}$$

3. Calculation results of TBCs

A typical microstructure of plasma sprayed TBCs from the cross-section view by scanning electron microscopy (SEM) is shown in Fig. 4. It includes yttria partially stabilized zirconia (YSZ) and defects. The model size is 120 μm × 90 μm within the total porosity fraction of 3.68%. In the present work, we only study the effects of defects on the effective thermal conductivity, so the only parameter which influences the effective properties is the defects system without considering the influences of interfaces, however, it is important to note that the splat interfaces are important contributors in defining the properties of coatings (see more discussion in [21]). With one pixel corresponding to one finite element, the collection of pixels can be changed to collection of finite elements. In this way, a finite element grid model with more than 40,000 quadrilateral elements in Fig. 5a based on the actual microstructure of TBCs is generated by digital image processing theory and finite element mesh generation principle [22]. In addition, the results of the effective thermal conductivity are obtained through the

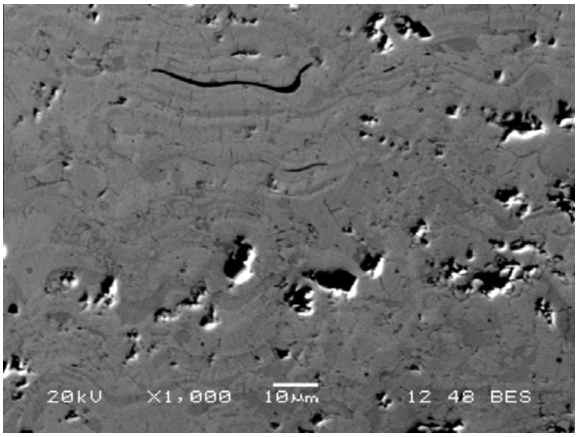

Fig. 4. The cross-section microstructure of TBCs (120 μm × 90 μm).

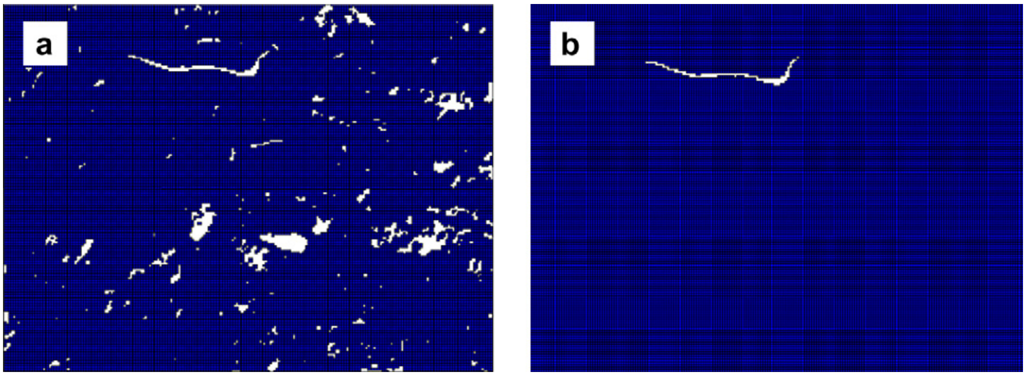

Fig. 5. The finite element grid model of TBCs with (a) all defects inside, $C_K = 1763\ \mu m^2$, $D = 2160\ \mu m^2$. (b) only No.1 defect inside, $C_K(1) = 956\ \mu m^2$, $D(1) = 956\ \mu m^2$.

steady-state heat transfer analysis. To obtain the effective thermal conductivity along the spray direction, a fixed temperature condition is prescribed in both the top and the bottom boundaries, and the other two boundaries are kept insulated. Additionally, the intrinsic thermal conductivity of the non-defective bulk material of YSZ material is $K_0 = 2.2$ W/mk. By employing FEM analyses in conjunction with Eq. (3), the effective thermal conductivity along the spray direction is calculated as $K_{eff} = 1.76$ W/mk.

Specify the longest transverse crack in Fig. 5b is the No.1 defect in Eq. (11), $C_K(1)$, which is with an approximate length of 35 μm. According to Eq. (19), $C_K(1)$ is given by

$$C_K(1) = \beta \cdot b^2 \approx 3.12 \times 17.5^2 = 956\ \mu m^2 \tag{26}$$

Then, Eq. (11) can be rewritten as

$$K_{eff} = K_0 \left[1 - \rho - \frac{C_K(1) + \sum_{i=2}^{n} C_K(i)}{hl} \right], \tag{27a}$$

$$1.76 = 2.2 \times \left[1 - 0.036 - \frac{956 + \sum_{i=2}^{n} C_K(i)}{90 \times 120} \right]. \tag{27b}$$

Thus,

$$\sum_{i=2}^{n} C_K(i) = 807\ \mu m^2. \tag{28}$$

The influence parameter of defects on the effective thermal conductivity of TBCs can be expressed as

$$D(1) = C_K(1) = 956\ \mu m^2, \tag{29a}$$

$$\sum_{2}^{n} D(i) = \sum_{i=2}^{n} C_K(i) + \rho \cdot (h \cdot l) = 1204\ \mu\mathrm{m}^2, \tag{29b}$$

$$D = D(1) + \sum_{2}^{n} D(i) = 2160\ \mu\mathrm{m}^2. \tag{29c}$$

$\sum_{i=2}^{n} D(i) > D(1)$, which indicates that the effect of the longest transverse crack is smaller than all the other defects combined together. However, the longest transverse crack still by all odds plays the most important role for the effective thermal conductivity of TBCs along the spray direction than any individual defect.

4. Conclusion

Based on the law of the conservation of energy, mathematical formulas of the effective in-plane thermal conductivity of TBCs are proposed.

(1) With the aid of strict analytical calculation, the contribution of defects on the effective thermal conductivity of TBCs is expressed as $D = \rho \cdot hl + \sum_{i=1}^{n} C_K(i)$, where C_K is an independent variation of thermal nonlinear area around the defect, which is only affected by the defect.

(2) By means of analytical mathematical formulations in conjunction with FEM results, C_K of pore with radius a is fitted as $C_K = \alpha \cdot a^2$, C_K of transverse crack with length $2b$ is fitted as $C_K = \beta \cdot b^2$.

(3) The effective thermal conductivity of plasma sprayed TBCs based on a typical actual microstructure is studied. The effects of defects on the effective thermal conductivity of TBCs is expressed by influence parameter clearly, which shows that the longest transverse crack plays the most important role for the effective thermal conductivity along the spray direction than any individual defect.

Acknowledgment

We acknowledge the funding supports of the project (No. 50801005) from the Chinese National Natural Science Foundation.

References

[1] Y. Sun, C. Eripret, G. Rousselier, Influence of defect shape on damage evolution and fracture behavior of ductile materials, Eng. Fract. Mech. 51 (1995) 337–347.
[2] Y.N. Podrezov, N.L. Lugovoi, V.N. Slyunyaev, Influence of random pore-type mesodefects on the strength of brittle materials, Powder Metall. Met. Ceram. 38 (1999) 198–201.
[3] J.W. Ju, T.M. Chen, Effective elastic moduli of two-phase composites containing randomly dispersed spherical inhomogeneities, Acta Mech. 103 (1994) 123–144.
[4] D.P.H. Hasselman, Effect of cracks on thermal comductivity, J. Comput. Materials 12 (1978) 403–406.
[5] D.P.H. Hasselma, J.P. Singh, Analysis of thermal stress resistance of microcracked brittle ceramics, Am. Ceram Soc. Bull 58 (1979) 856–860.
[6] R. McPherson, A model for the thermal conductivity of plasma sprayed ceramic coatings, Thin Solid Films 112 (1984) 89–95.
[7] K. Markov, L. Preziosi, Heterogeneous media: micromechanics modeling methods and simulations. Birkhäuser Boston: c/o Springer-Verlag New York, Inc, 1999.
[8] J.R. Nicholls, K.J. Lawson, A. Johnstone, D.S. Rickerby, Methods to reduce the thermal conductivity of EB-PVD TBCs, Surf. Coat. Technol. 151–152 (2002) 383–391.
[9] S.Y. Lu, J.L. Song, Effective conductivity of composites with spherical inclusions: Effect of coating and detachment, J. Appl. Phys. 79 (1996) 609–618.
[10] I. Sevostianov, M. Kachanov, Plasma-sprayed ceramic coatings: anisotropic elastic and conductive properties in relation to the microstructure; cross-property correlations, Mater. Sci. Eng.: A 297 (2001) 235–243.
[11] K.W. Schlichting, N.P. Padture, P.G. Klemens, Thermal conductivity of dense and porous yttria-stabilized zirconia, J. Mater. Sci. 36 (2001) 3003–3010.
[12] D.R. Clarke, Materials selection guidelines for low thermal conductivity thermal barrier coatings, Surf. Coat. Technol. 163–164 (2003) 67–74.
[13] Z. Wang, A. Kulkarni, S. Deshpande, T. Nakamura, H. Herman, Effects of pores and interfaces on effective properties of plasma sprayed zirconia coatings, Acta Mater. 51 (2003) 5319–5334.
[14] F. Cernuschi, P.G. Bison, S. Marinetti, P. Scardi, Thermophysical, mechanical and microstructural characterization of aged free-standing plasma-sprayed zirconia coatings, Acta Mater. 56 (2008) 4477–4488.
[15] K.A. Khor, Y.W. Gu, Thermal properties of plasma-sprayed functionally graded thermal barrier coatings, Thin Solid Films 372 (2000) 104–113.
[16] D.D. Hass, A.J. Slifka, H.N. Wadley, Low thermal conductivity vapor deposited zirconia microstructures, Acta Mater. 49 (2001) 973–983.
[17] J. Wu, X. Wei, N.P. Padture, P.G. Klemens, M. Gell, Eugenio García, P. Miranzo, M.I. Osendi, Low-thermal-conductivity rare-earth zirconates for potential thermal-barrier-coating applications, J. Am. Ceram. Soc. 85 (2002) 3031–3035.
[18] P. Michlik, C. Berndt, Image-based extended finite element modeling of thermal barrier coatings, Surf. Coat. Technol. 201 (2006) 2369–2380.
[19] A.D. Jadhav, N.P. Padture, E.H. Jordan, M. Gell, P. Miranzo, J.E. Fuller, Low-thermal-conductivity plasma-sprayed thermal barrier coatings with engineered microstructures, Acta Mater. 54 (2006) 3343–3349.
[20] S. A. Langer, W. C. Carter, E. R. Fuller, Object Oriented Finite Element Analysis for Materials Science, Center for Theoretical and computational Materials Science and the Information Lab. at the NIST, 1997, URL: www.ctcms.nist.gov/oof/ (10/2004).
[21] S. Wei, W. Fu-chi, F. Qun-bo, H. Dan, M. Zhuang, Proposal of new expressions for effects of splat interfaces and defects on the effective properties of thermal barrier coatings, Surf. Coat. Technol. 204 (2010) 3376–3381.
[22] S. Wei, F. Qun-bo, W. Fu-chi, M. Zhuang, Modeling of micro-crack growth during thermal shock based on microstructural images of thermal barrier coatings, Comput. Mater. Sci. 49 (2009) 600–602.